Nickel Based Brazes for Planar Solid Oxide Fuel Cell Applications

Quan Zhou, Yuxi Ma, Tridip Das, Dr. Yue Qi, Dr. Jason D. Nicholas, Dr. Thomas R. Bieler
Department of Chemical Engineering and Materials Science
Michigan State University, East Lansing, MI 48824-1226 , zhouqua3@egr.msu.edu

Introduction

Solid oxide fuel cells (SOFCs) are power generation devices that can convert the chemical energy from a wide range of fuels and energy-carriers directly into electricity with high efficiency [1]. However, one of the major challenges for the viability of commercial SOFC devices is the development of suitable sealing technologies for the long-term separation of the air and fuel in the system at high temperature (~750^{0}C).

The solution that is widely utilized in industry is the reactive air brazing (RAB) of Ag-based brazes. However, due to the inherent high diffusivity of both H_2 and O_2 in silver (Figure 1a) [2], the diffused H_2 and O_2 react to form micro-pores in the braze matrix (Figure 1b) that eventually degrade the seal, reduce the mechanical robustness of the joint, and limit the lifetime of commercial SOFC devices to ~10,000 hours [3].

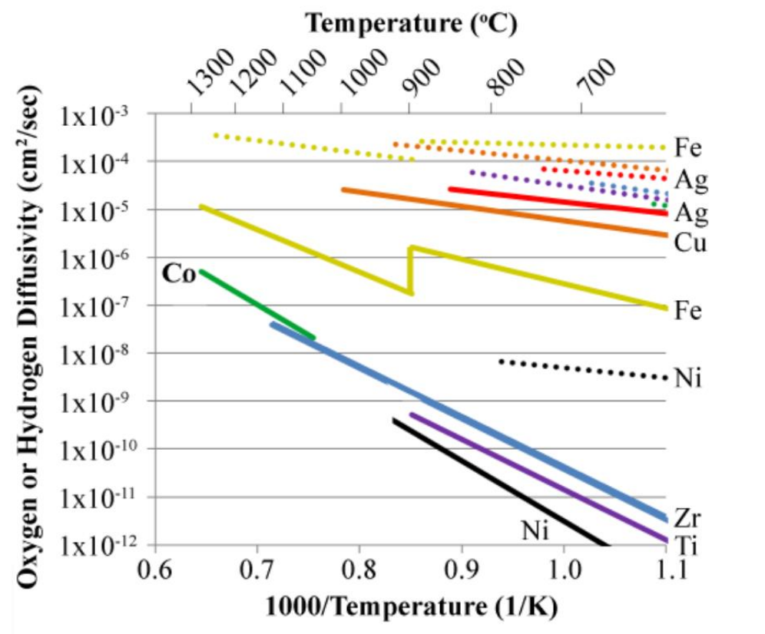

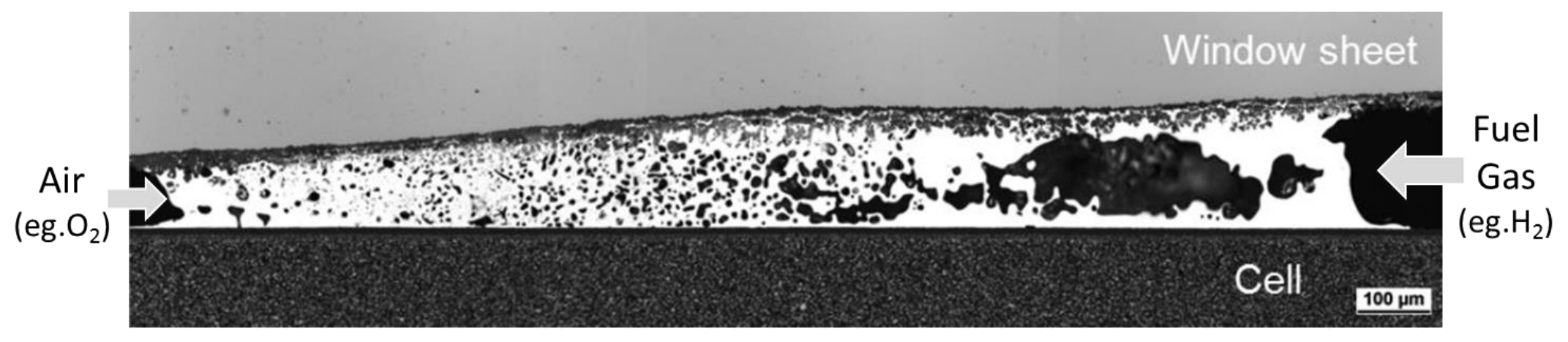

Figure 1. (a) (left) __Oxygen (solid)__ & __Hydrogen (dotted)__ diffusivities in several common metals [2]; (b) (above) Cross-section showing micro-pores in an Ag based braze [3]

Proposed Strategy

Here, a computationally aided approach is proposed to design a new, self-passivating braze that will be suitable to replace the current Ag-based braze and prolong the lifetime of SOFC devices.

Table I. Braze requirements

Design Parameter	Target Values	Justification
Solidus Temperature (Ts)	900°C ≤ Ts≤ 1015°C	So the braze is solid during SOFC operation & does not alter the microstructure of previously made layers
Oxidation Resistance	No oxidation or limited oxidation before passivating surface oxide is formed	To ensure a stable joint, also to prevent O_2 from getting into the braze
Wetting (θ) and Bonding on Both Faying Surfaces	0° ≤ θ ≤ 60°; Interdiffusion or new phase formation	To ensure that the braze spreads through the joint and forms good bonding at both interfaces
Mechanical Stability	Sufficient Ductility or Compatible CTE	To maintain mechanical robustness during longterm SOFC application and thermal cycling

- Computationally identify candidate alloy systems with acceptable melting ranges.
- Physically fabricate candidate alloys and perform characterization with various techniques.

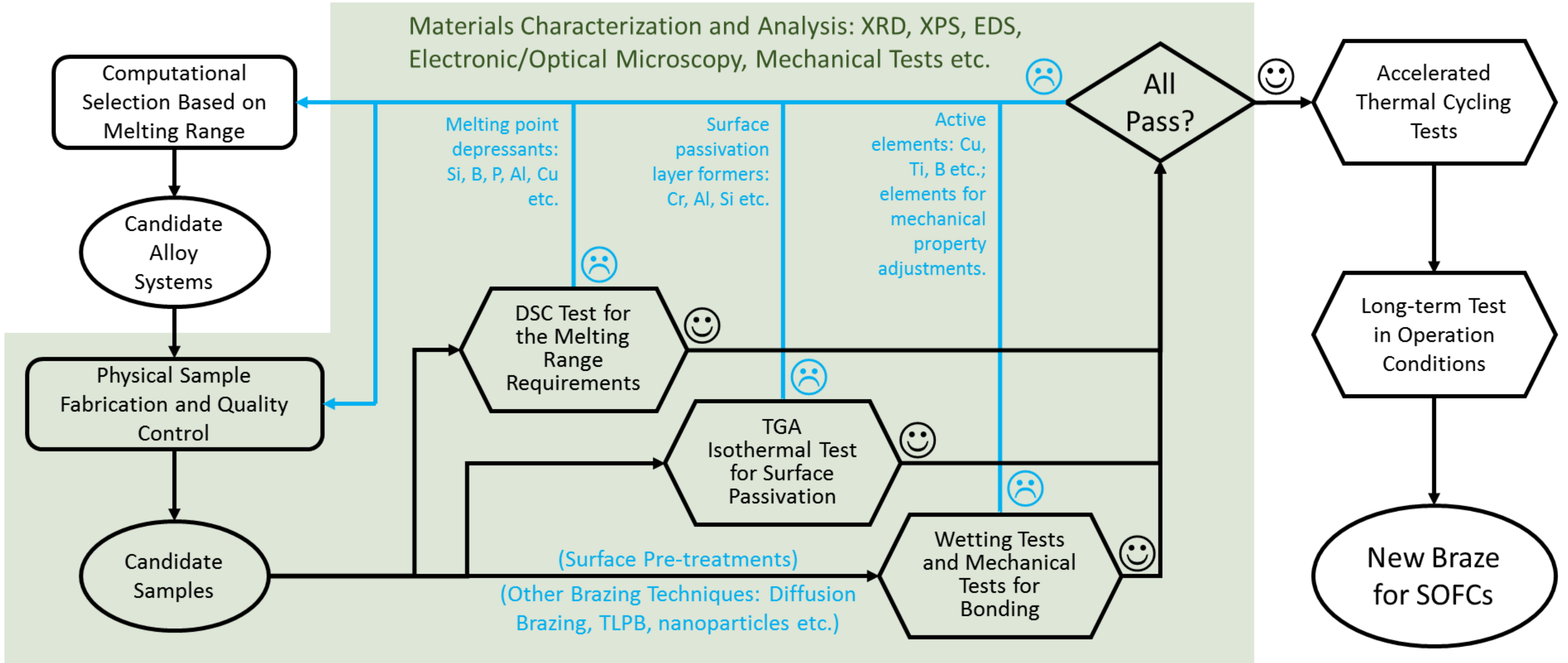
Materials Characterization and Analysis: XRD, XPS, EDS, Electronic/Optical Microscopy, Mechanical Tests etc.

Computational Selection Based on Melting Range

Candidate Alloy Systems

Physical Sample Fabrication and Quality Control

Candidate Samples

Melting point depressants: Si, B, P, Al, Cu etc.

Surface passivation layer formers: Cr, Al, Si etc.

Active elements: Cu, Ti, B etc.; elements for mechanical property adjustments.

DSC Test for the Melting Range Requirements

TGA Isothermal Test for Surface Passivation

Wetting Tests and Mechanical Tests for Bonding

(Surface Pre-treatments)

(Other Brazing Techniques: Diffusion Brazing, TLPB, nanoparticles etc.)

All Pass?

Accelerated Thermal Cycling Tests

Long-term Test in Operation Conditions

New Braze for SOFCs

Figure 2. Design strategy flowchart

Computationally Identified Braze Compositions

The Thermo-Calc© software was used to find candidate alloy systems within the target melting range for the brazing application. Alloy systems in green boxes below are promising candidates (Green indicates candidate alloys within liquidus and solidus temperature in the target range).

Table II. Candidate Ni-based Alloy Systems

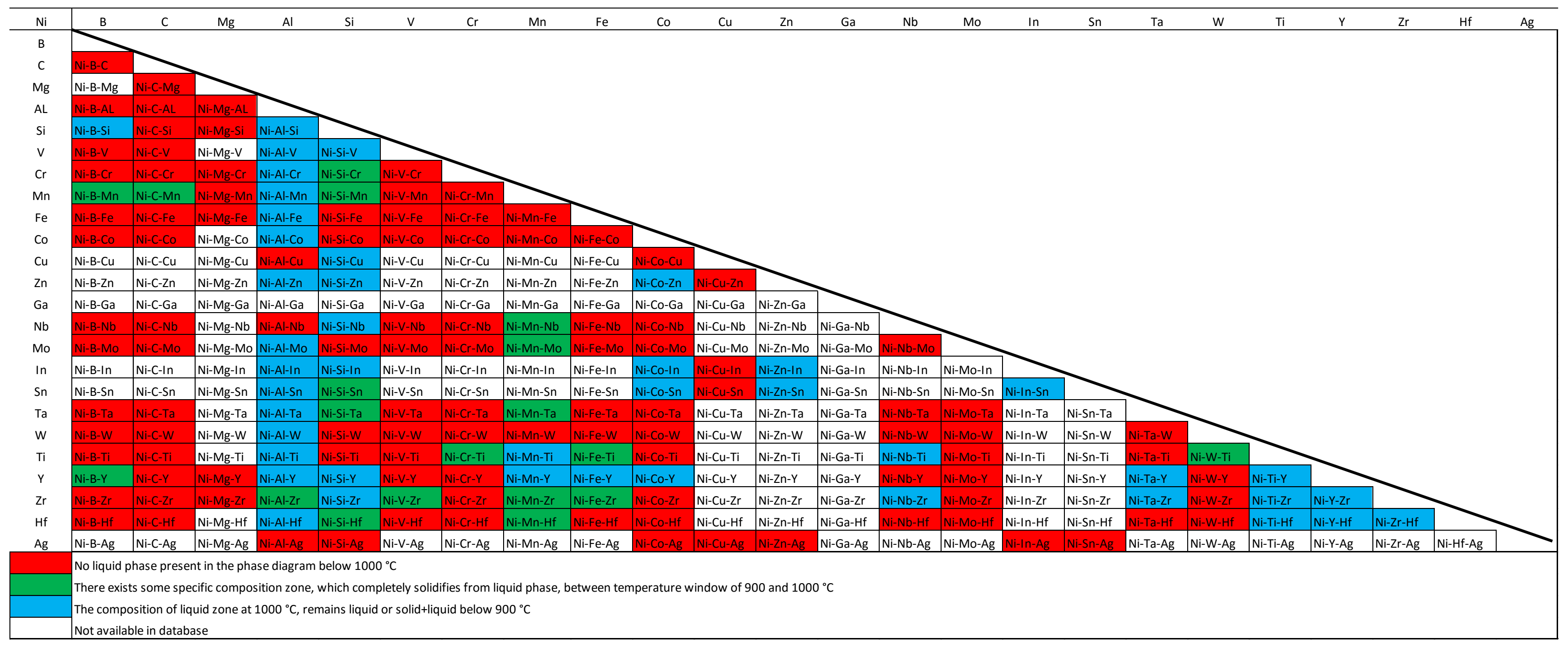

Ni	B	C	Mg	Al	Si	V	Cr	Mn	Fe	Co	Cu	Zn	Ga	Nb	Mo	In	Sn	Ta	W	Ti	Y	Zr	Hf	Ag
B																								
C	🟥 Ni-B-C																							
Mg	Ni-B-Mg	🟥 Ni-C-Mg																						
AL	🟥 Ni-B-AL	🟥 Ni-C-AL	🟥 Ni-Mg-AL																					
Si	🟦 Ni-B-Si	🟥 Ni-C-Si	🟥 Ni-Mg-Si	🟦 Ni-Al-Si																				
V	🟥 Ni-B-V	🟥 Ni-C-V	Ni-Mg-V	🟦 Ni-Al-V	🟦 Ni-Si-V																			
Cr	🟥 Ni-B-Cr	🟥 Ni-C-Cr	🟥 Ni-Mg-Cr	🟦 Ni-Al-Cr	🟩 Ni-Si-Cr	🟥 Ni-V-Cr																		
Mn	🟩 Ni-B-Mn	🟩 Ni-C-Mn	🟥 Ni-Mg-Mn	🟦 Ni-Al-Mn	🟩 Ni-Si-Mn	🟥 Ni-V-Mn	🟥 Ni-Cr-Mn																	
Fe	🟥 Ni-B-Fe	🟥 Ni-C-Fe	🟥 Ni-Mg-Fe	🟦 Ni-Al-Fe	🟥 Ni-Si-Fe	🟥 Ni-V-Fe	🟥 Ni-Cr-Fe	🟥 Ni-Mn-Fe																
Co	🟥 Ni-B-Co	🟥 Ni-C-Co	Ni-Mg-Co	🟦 Ni-Al-Co	🟥 Ni-Si-Co	🟥 Ni-V-Co	🟥 Ni-Cr-Co	🟥 Ni-Mn-Co	🟥 Ni-Fe-Co															
Cu	Ni-B-Cu	Ni-C-Cu	Ni-Mg-Cu	🟥 Ni-Al-Cu	🟦 Ni-Si-Cu	Ni-V-Cu	Ni-Cr-Cu	Ni-Mn-Cu	Ni-Fe-Cu	🟥 Ni-Co-Cu														
Zn	Ni-B-Zn	Ni-C-Zn	Ni-Mg-Zn	🟦 Ni-Al-Zn	🟦 Ni-Si-Zn	Ni-V-Zn	Ni-Cr-Zn	Ni-Mn-Zn	Ni-Fe-Zn	🟦 Ni-Co-Zn	🟥 Ni-Cu-Zn													
Ga	Ni-B-Ga	Ni-C-Ga	Ni-Mg-Ga	Ni-Al-Ga	Ni-Si-Ga	Ni-V-Ga	Ni-Cr-Ga	Ni-Mn-Ga	Ni-Fe-Ga	Ni-Co-Ga	Ni-Cu-Ga	Ni-Zn-Ga												
Nb	🟥 Ni-B-Nb	🟥 Ni-C-Nb	Ni-Mg-Nb	🟥 Ni-Al-Nb	🟦 Ni-Si-Nb	🟥 Ni-V-Nb	🟥 Ni-Cr-Nb	🟩 Ni-Mn-Nb	🟥 Ni-Fe-Nb	🟥 Ni-Co-Nb	Ni-Cu-Nb	Ni-Zn-Nb	Ni-Ga-Nb											
Mo	🟥 Ni-B-Mo	🟥 Ni-C-Mo	Ni-Mg-Mo	🟦 Ni-Al-Mo	🟥 Ni-Si-Mo	🟥 Ni-V-Mo	🟥 Ni-Cr-Mo	🟩 Ni-Mn-Mo	🟥 Ni-Fe-Mo	🟥 Ni-Co-Mo	Ni-Cu-Mo	Ni-Zn-Mo	Ni-Ga-Mo	🟥 Ni-Nb-Mo										
In	Ni-B-In	Ni-C-In	Ni-Mg-In	🟦 Ni-Al-In	🟦 Ni-Si-In	Ni-V-In	Ni-Cr-In	Ni-Mn-In	Ni-Fe-In	🟦 Ni-Co-In	🟥 Ni-Cu-In	🟦 Ni-Zn-In	Ni-Ga-In	Ni-Nb-In	Ni-Mo-In									
Sn	Ni-B-Sn	Ni-C-Sn	Ni-Mg-Sn	🟦 Ni-Al-Sn	🟩 Ni-Si-Sn	Ni-V-Sn	Ni-Cr-Sn	Ni-Mn-Sn	Ni-Fe-Sn	🟦 Ni-Co-Sn	🟥 Ni-Cu-Sn	🟦 Ni-Zn-Sn	Ni-Ga-Sn	Ni-Nb-Sn	Ni-Mo-Sn	🟦 Ni-In-Sn								
Ta	🟥 Ni-B-Ta	🟥 Ni-C-Ta	Ni-Mg-Ta	🟦 Ni-Al-Ta	🟩 Ni-Si-Ta	🟥 Ni-V-Ta	🟥 Ni-Cr-Ta	🟩 Ni-Mn-Ta	🟥 Ni-Fe-Ta	🟥 Ni-Co-Ta	Ni-Cu-Ta	Ni-Zn-Ta	Ni-Ga-Ta	🟥 Ni-Nb-Ta	🟥 Ni-Mo-Ta	Ni-In-Ta	Ni-Sn-Ta							
W	🟥 Ni-B-W	🟥 Ni-C-W	Ni-Mg-W	🟦 Ni-Al-W	🟥 Ni-Si-W	🟥 Ni-V-W	🟥 Ni-Cr-W	🟥 Ni-Mn-W	🟥 Ni-Fe-W	🟥 Ni-Co-W	Ni-Cu-W	Ni-Zn-W	Ni-Ga-W	🟥 Ni-Nb-W	🟥 Ni-Mo-W	Ni-In-W	Ni-Sn-W	🟥 Ni-Ta-W						
Ti	🟥 Ni-B-Ti	🟥 Ni-C-Ti	Ni-Mg-Ti	🟦 Ni-Al-Ti	🟥 Ni-Si-Ti	🟥 Ni-V-Ti	🟩 Ni-Cr-Ti	🟦 Ni-Mn-Ti	🟩 Ni-Fe-Ti	🟥 Ni-Co-Ti	Ni-Cu-Ti	Ni-Zn-Ti	Ni-Ga-Ti	🟦 Ni-Nb-Ti	🟥 Ni-Mo-Ti	Ni-In-Ti	Ni-Sn-Ti	🟥 Ni-Ta-Ti	🟩 Ni-W-Ti					
Y	🟩 Ni-B-Y	🟥 Ni-C-Y	🟥 Ni-Mg-Y	🟦 Ni-Al-Y	🟦 Ni-Si-Y	🟥 Ni-V-Y	🟥 Ni-Cr-Y	🟦 Ni-Mn-Y	🟦 Ni-Fe-Y	🟦 Ni-Co-Y	Ni-Cu-Y	Ni-Zn-Y	Ni-Ga-Y	🟥 Ni-Nb-Y	🟥 Ni-Mo-Y	Ni-In-Y	Ni-Sn-Y	🟦 Ni-Ta-Y	🟥 Ni-W-Y	🟦 Ni-Ti-Y				
Zr	🟥 Ni-B-Zr	🟥 Ni-C-Zr	🟥 Ni-Mg-Zr	🟩 Ni-Al-Zr	🟦 Ni-Si-Zr	🟩 Ni-V-Zr	🟥 Ni-Cr-Zr	🟩 Ni-Mn-Zr	🟩 Ni-Fe-Zr	🟥 Ni-Co-Zr	Ni-Cu-Zr	Ni-Zn-Zr	Ni-Ga-Zr	🟦 Ni-Nb-Zr	🟥 Ni-Mo-Zr	Ni-In-Zr	Ni-Sn-Zr	🟦 Ni-Ta-Zr	🟥 Ni-W-Zr	🟦 Ni-Ti-Zr	🟦 Ni-Y-Zr			
Hf	🟥 Ni-B-Hf	🟥 Ni-C-Hf	Ni-Mg-Hf	🟦 Ni-Al-Hf	🟩 Ni-Si-Hf	🟥 Ni-V-Hf	🟥 Ni-Cr-Hf	🟩 Ni-Mn-Hf	🟥 Ni-Fe-Hf	🟥 Ni-Co-Hf	Ni-Cu-Hf	Ni-Zn-Hf	Ni-Ga-Hf	🟥 Ni-Nb-Hf	🟥 Ni-Mo-Hf	Ni-In-Hf	Ni-Sn-Hf	🟥 Ni-Ta-Hf	🟥 Ni-W-Hf	🟦 Ni-Ti-Hf	🟦 Ni-Y-Hf	🟦 Ni-Zr-Hf		
Ag	Ni-B-Ag	Ni-C-Ag	Ni-Mg-Ag	🟥 Ni-Al-Ag	🟥 Ni-Si-Ag	Ni-V-Ag	Ni-Cr-Ag	Ni-Mn-Ag	Ni-Fe-Ag	🟥 Ni-Co-Ag	🟥 Ni-Cu-Ag	🟥 Ni-Zn-Ag	Ni-Ga-Ag	Ni-Nb-Ag	Ni-Mo-Ag	🟥 Ni-In-Ag	🟥 Ni-Sn-Ag	Ni-Ta-Ag	Ni-W-Ag	Ni-Ti-Ag	Ni-Y-Ag	Ni-Zr-Ag	Ni-Hf-Ag	

🟥	No liquid phase present in the phase diagram below 1000 °C
🟩	There exists some specific composition zone, which completely solidifies from liquid phase, between temperature window of 900 and 1000 °C
🟦	The composition of liquid zone at 1000 °C, remains liquid or solid+liquid below 900 °C
⬜	Not available in database

Melting Point and Oxidation Behavior I

The above candidates were fabricated through arc-melting and examined with energy dispersive X-ray spectroscopy (EDS) for chemical homogeneity; then mechanically sectioned for further testing. Thermogravimetric analysis (TGA) were performed in air at 750 ^{0}C to quickly identify alloys with superior oxidation resistance. Differential scanning calorimetry (DSC) was also performed to measure the melting range of candidate alloys. A representative DSC calibration test and sample melting point determination are shown in Fig. 3. Additional preliminary results are summarized in Table III where green (red) indicate alloys that met (did not meet) the design criteria.

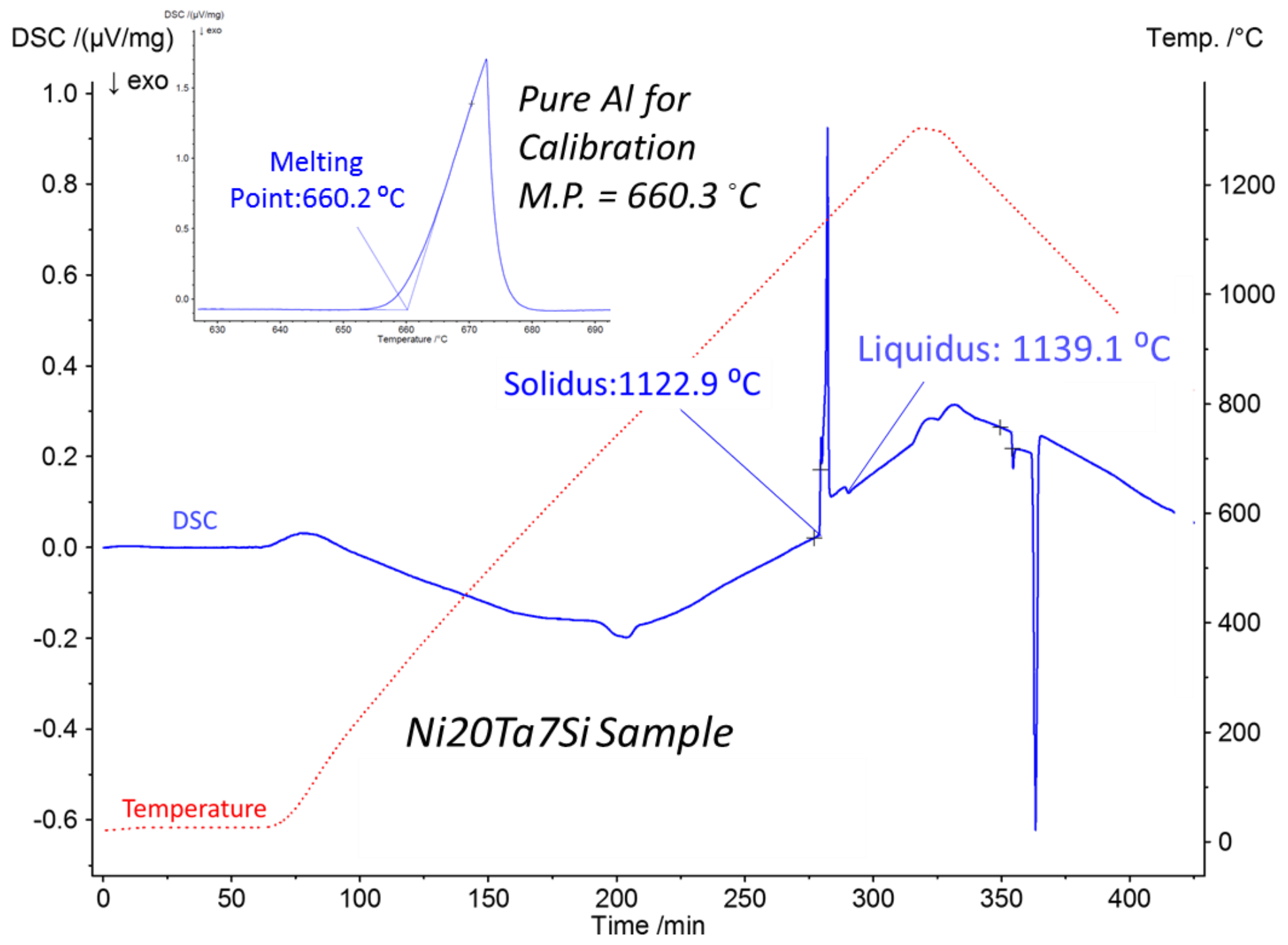

Figure 3. Example DSC measurement and calibration

Table III. DSC Results and Preliminary Oxidation Resistance for Ni-based Braze Alloys

Alloy Composition	48 hr 750°C Oxidation Resistance in Air	Solidus Temperature	Liquidus Temperature
Ni43.5Mn14.8Nb	Poor		
Ni48.5Mn14.6Mo	Poor		
Ni50Mn5Si	Poor		
Ni36.9Mn11Si			
Ni52.2Mn10.9Ta	Poor		
Ni26.0Mn22.4Si			
Ni4.5Si7.0Cr (B, Fe Free BNi2)	Excellent	Excellent	Excellent
Ni4.5Si7.0Cr3.1B3.0Fe (Commercial BNi2 Containing Iron)	Excellent	Excellent	Excellent
Ni5Si2Cr60Al			
Ni5Si20Ta	Poor	Too High (1132.1)	Too High (1138.0)
Ni7Si20Ta	Good	Too High (1122.9)	Too High (1139.1)
Ni7Si20Ta1B	Good	Good (1057.6)	Good (1068.0)
Ni7Si20Ta3B	Good	Good (1059.6)	Good (1086.8)
Ni10Si20Ta	Excellent	Too High (1124.1)	Too High (1162.9)
Ni7Si32Ta1B	Good	Good (1059.3)	Good (1070.1)
Ni7Si32Ta	Marginal	Too High (1125.4)	Too High (1146.1)
Ni7Si25Ta		Too High (1124.5)	Too High (1137.9)
Ni7Si10Ta		Too High (1127.4)	Too High (1140.3)
Ni71.5Ti	Extremely Poor		
Ni41Ti17Nb2Al	Fair		
Ni41Ti17Nb3Al	Poor		
Ni41Ti17Nb5Al	Fair		
Ni42.5Zr2Al3.5Si	Poor		
Ni9Zr11Nb4Si	Poor		
Ni35Zr13.3Y	Extremely Poor		
Ti15Ni15Fe	Poor	Good (1007.2)	Good (1037.7)
Ti32Ni8Cr	Poor	Good (975.5)	Good (1025.1)
Ni17Zr5.5Al	Poor	Too High (1207.4)	Too High (1221.4.4)
Ni15Zr3.5Si2Al	Poor	Good (1060.4)	Good (1066.2)
Ni30In5Zn	Good	Good (917.1)	Good (923.1)
Ni41.4In (eutectic)	Good	Good (916.0)	Good (926.2)
Ni10Ta7Si1B		Good (1033.7)	Good (1074.3)
Ni10Si	Excellent	Too High (1126.5)	Too High (1222.5)
Ni10Si1B	Excellent	Good (992.0)	Good (1032.8)
Ni7Ta2Si	Marginal		

Melting Point and Oxidation Behavior II

Figure 4a shows the TGA results of some Ni-Si(Ta,B) alloys. The Ni-10Si(B) samples showed better oxidation resistance than the commercial BNi2 braze. Increased Ta additions degrade the oxidation resistance, but successfully reduce the liquidus temperature of Ni-10Si alloy by ~60 ^{0}C. Also, with 1 wt.% B addition, the Ni20Ta7Si1B sample showed interesting oxidation mechanism that may provide passivation.

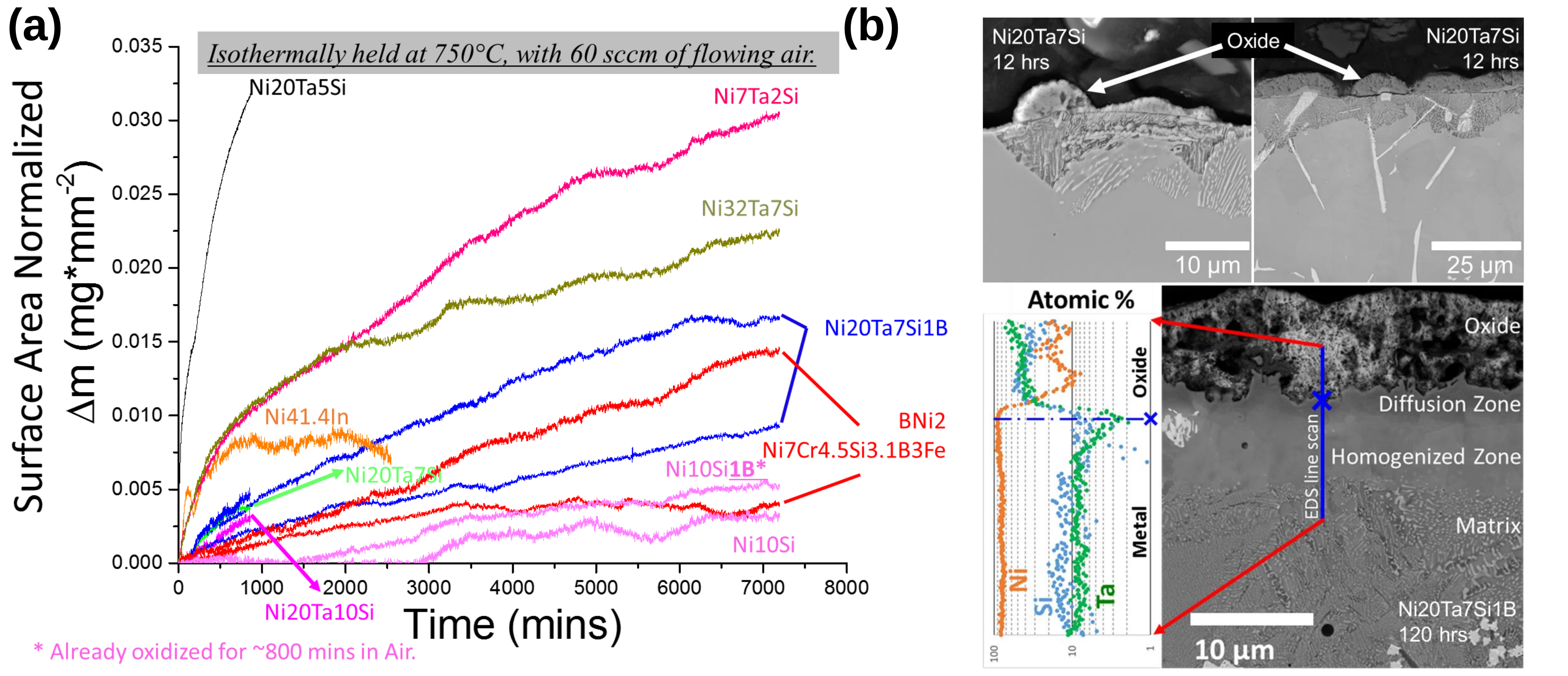

Figure 4. (a) Surface area normalized weight gain of different samples at 750 ℃ in air; (b) Backscatter electron images (BSE) of TGA tested sample cross-sections

Wetting and Braze Joint Manufacture

Fig. 5a and 5b shows that the wetting of Ni-based braze materials on different substrates as well as Cu on YSZ. Here a multilayered brazing method is explored and a braze joint was successfully produced as shown in Fig 5c. Optimization of this design regarding materials selection, layer thickness and surface pre-treatments is underway.

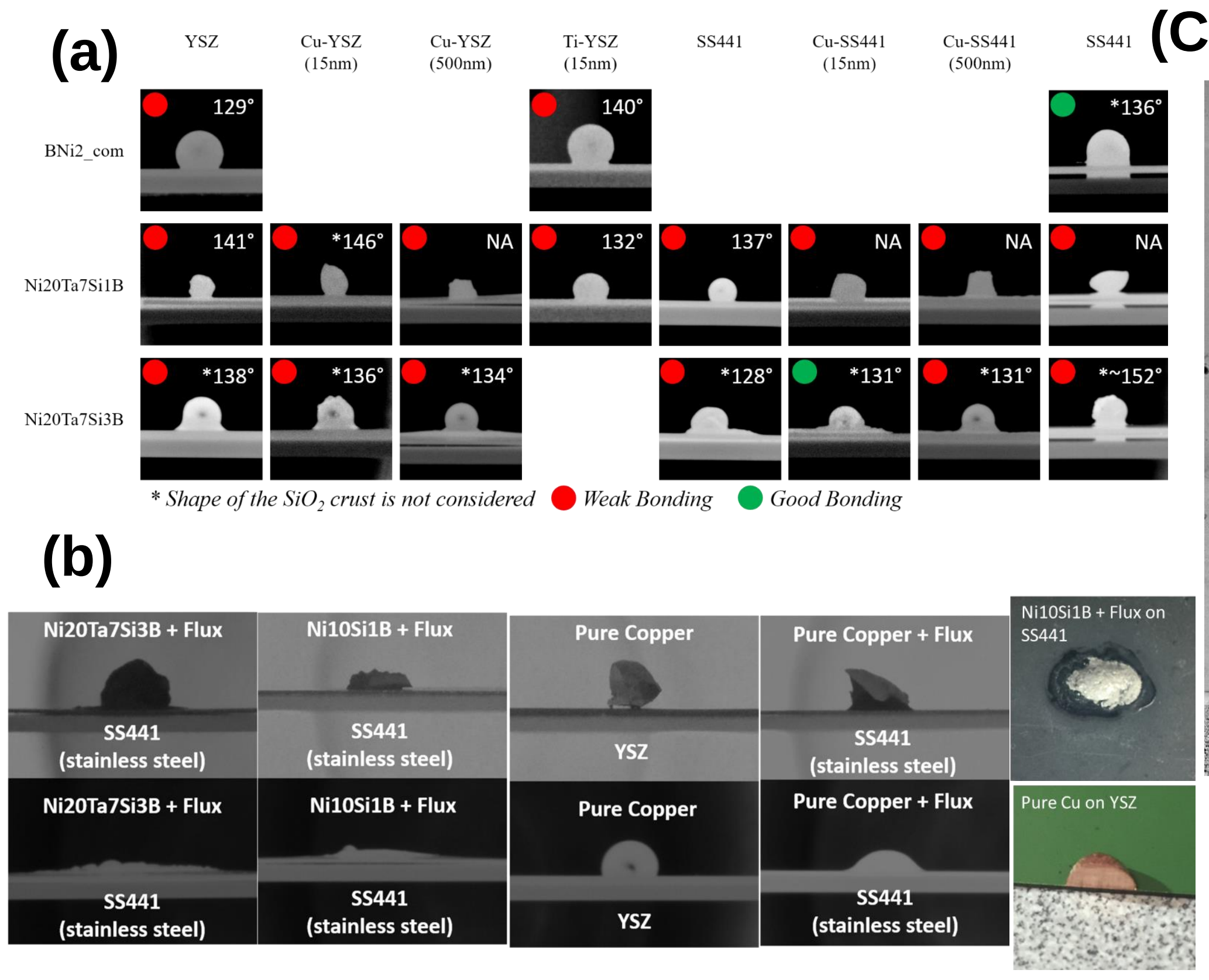

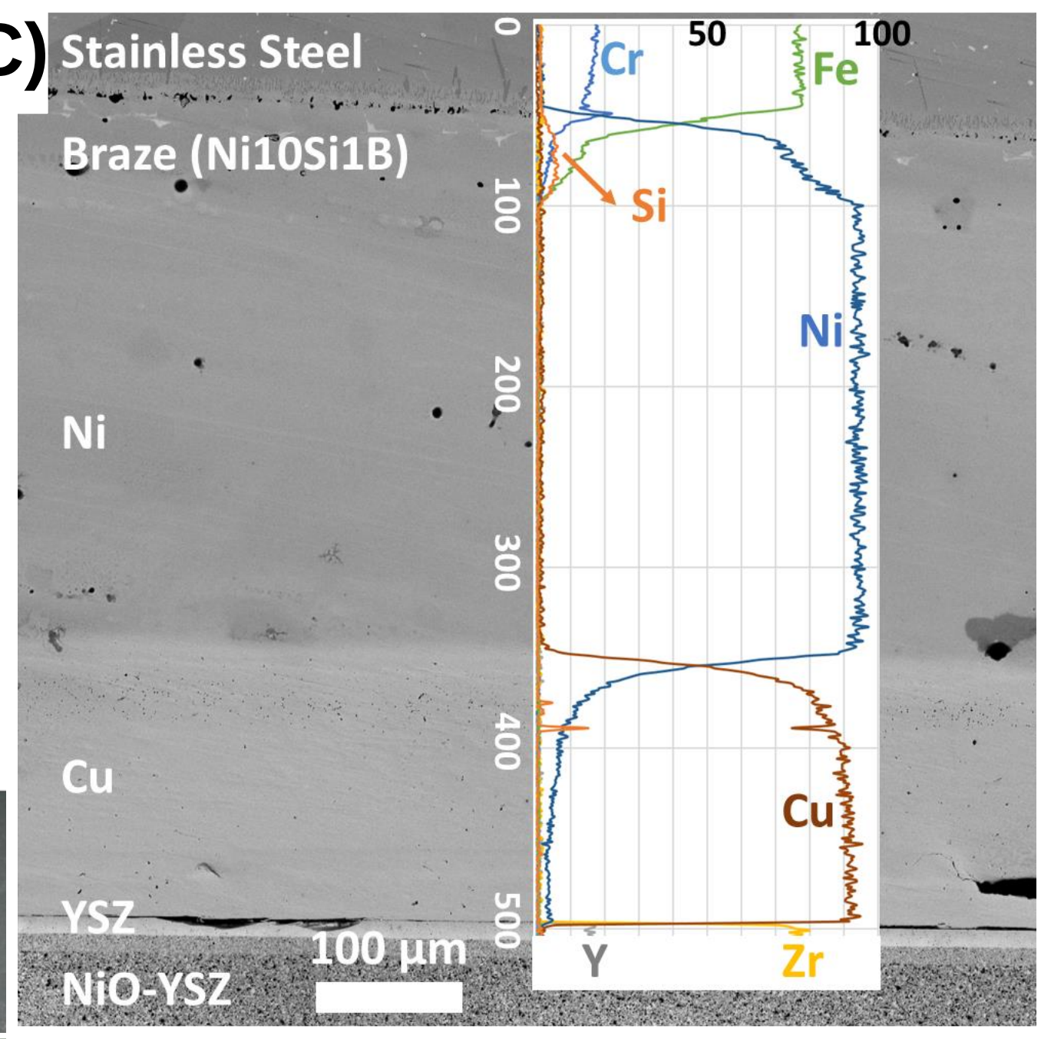

Figure 5. Wetting test results (a) without flux and (b) with flux; (c) BSE image of a multilayered braze joint with an EDS line scan.

Conclusion

1. A systematic computation-experiment approach was developed to search for, fabricate, and characterize braze alloys for SOFC application.
2. A new multilayered brazing method was explored using a multilayered approach and a joint was successfully produced.

Acknowledgement: This material is based upon work supported by the Department of Energy under Award Number DE-FE0023315.

References

[1] Wachsman, E.D. and K.T. Lee, Lowering the Temperature of Solid Oxide Fuel Cells. ***Science***, (2011).
[2] C. Smithells, W. Gale, T. Totemeier. ***Smithells Metals Reference Book***. 8th ed.
[3] Bause, T., et al., Damage and Failure of Silver Based Ceramic/Metal Joints for SOFC Stacks. ***Fuel Cells***, (2013).